Mineralogy, fluid inclusions and stable isotope study of epithermal Au-Ag-Bi-Te mineralization from the SE Afar Rift (Djibouti)

N. Moussa, Marie-Christine Boiron, N.V. Grassineau, D. Asael, Y. Fouquet, B. Le Gall, Joël Rolet, J. Etoubleau, Christophe Delacourt

Ore Geology Reviews
August 2019, Volume 111, Pages 102916 (14p.)
https://doi.org/10.1016/j.oregeorev.2019.05.002
https://archimer.ifremer.fr/doc/00494/60528/

Mineralogy, fluid inclusions and stable isotope study of epithermal Au-Ag-Bi-Te mineralization from the SE Afar Rift (Djibouti)

Moussa N. [1, 2, 3, *], Boiron M.C- [4], Grassineau N.V. [5], Asael Dan [6], Fouquet Yves [2], Le Gall Bernard [3], Rolet Joël [3], Etoubleau Joel [2], Delacourt Christophe [3]

[1] IST, Centre d'Etudes et de Recherches de Djibouti, B.P. 486, Djibouti
[2] IFREMER, Centre de Brest, BP 70, 29280 Plouzané, France
[3] UMR/CNRS 6538 Géosciences Océan, UBO-IUEM, Place Nicolas Copernic, 29280, Plouzané, France
[4] GéoRessources, Université de Lorraine, CNRS, CREGU, Boulevard des Aiguillettes, B.P. 70239, F-54506, Vandœuvre-lès-Nancy, France
[5] Department of Earth Sciences, Royal Holloway University of London, EGHAM Surrey TW20 0EX, UK
[6] Department of Geology and Geophysics, Yale University, New Haven, CT 06520, USA

* Corresponding author : N. Moussa, email address : nmoussae@gmail.com

Abstract :

In this paper, the mineralogy, fluid inclusions and stable isotopes of hydrothermal veins from the SE part of the Afar Rift (Djibouti) were studied. Mineralization occurs as gold-silver in quartz/carbonate veins and is mainly associated with felsic volcanism. The morphologies and textures of quartz show crustiform colloform banding, massive and breccias. Microthermometric measurements were made on quartz-hosted two phases (liquid + vapor) inclusions. Mean homogenization temperature ranges from 150°C to 340°C and ice-melting temperatures range from -0.2°C to - 1.6°C indicating that inclusion solutions contain 0.35 to 2.7 eq. wt. % NaCl. Furthermore, δ18O and δ13C values from calcite range from 3.7 to 26.6 ‰ and -7.5 to 0.3 ‰, respectively. The presence of platy calcite and adularia are consistent with boiling conditions. Our study shows that the deposit of precious-metal deposition occurred at around 250°C and is linked to a fluid generated by the mixture of magmatic fluid, hydrothermal fluid and seawater.

Graphical abstract

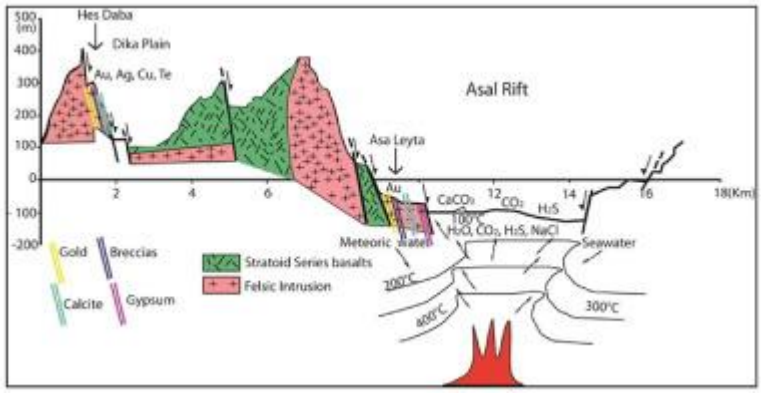

Highlights

► Au-Ag-Bi-Te minerals deposits on the edge of the Asal rift system (Djibouti) ► Microthermometric measurements and stable isotopes (C, O) were made on hydrothermal veins (e.g. quartz and carbonate veins) from the SE Afar Rift (Djibouti). ► Mean homogenization temperature ranges from 150°C to 340°C and ice-melting temperatures range from -0.2° to - 1.6°C and contain 0.35 to 2.7 eq. wt. % NaCl. ► $\delta^{18}O$ and $\delta^{13}C$ values from calcite range from 3.7 to 26.6 ‰ and -7.5 to 0.3‰, respectively. ► The most common textures of quartz are microcrystalline, jigsaw, plumose, crustiform and colloform. ► Three types of fluids have been identified in the SE Afar Rift: magmatic, meteoric and seawater fluids.

Keywords : Fluid inclusions, Stable Isotopes, Hydrothermal, Epithermal system, SE Afar Rift, Djibouti

1. Introduction

The Republic of Djibouti is located in the SE part of the Afar rift system, which is at the triple junction between the onshore prolongation of the Red Sea and the Gulf of Aden oceanic ridges and the Main Ethiopian continental rift (Fig. 1A). With regards to the Afar extensional context, Djibouti benefits from an exceptional geological setting, since it is the only place where most of the in the last ca. 30 Ma rift records (dominantly volcanic) are nearly continuously exposed above Mesozoic basement terrains that are also observed in the Ali Sabieh antiformal area to the south (Le Gall et al., 2010) (Fig. 1B). In addition, as extending onshore in the direct prolongation of the offshore Aden-Tadjoura accretionary ridge (Manighetti, 2004), the Asal tectono-magmatic active axis is generally thought to currently record incipient continental rupturing (Doubre et al., 2007). As such, it has been the focus of intense geological and geophysical investigations that resulted in a number of propagation rift models principally devoted to the last myrs rift history in SE Afar (Manighetti et al., 1997; Audin et al., 2001; Daoud et al., 2011). These tectono-magmatic models have been recently completed by integrating hydrothermal aspects that emphasized the role of dominantly magma-related fluids in the occurrence of epithermal ore deposits (Moussa et al. 2012; 2017). These occurrences are mainly represented by base metal and precious metals-bearing quartz/carbonate ±adularia veins (Moussa et al., 2012). High gold content have been identified in four different sites (Ali Addé, Arta, Hes Daba and Asa Leyta) (Fig.1B). However, temperature formation of ore deposits in Djibouti rift system has not been so far obtained. Only measured temperatures are known in the producing zones (260 to 359°C) during the geothermal exploration in the Asal Rift in 1987-1988 (D'Armore et al., 1998).

The knowledge of the circulation of fluid pathways in the crust began with research into the chemical compositions of hydrothermal fluids, the style of processes and the conditions of ore deposits (Potty et al., 1974; Wilkinson 2001; Samson et al., 2003). The study of fluid

inclusion in quartz and carbonate veins further allows to infer the paleo-environment of the hydrothermal systems (Bodnar et al., 1985). In fossil and active epithermal systems, studies of fluid inclusions show the relationships between fluids compositions and deposition of precious metals (Bodnar et al., 1985; Cathelineau et al., 1991; Mavrogenes et al., 1995; Hedenquist et al., 2000; Simmons et al., 2005; Moncada et al., 2012). Thus, the characteristic of fluid inclusions is an important guide both for the knowledge of processes controlling metal depositions and for exploration issues. However, a major problem is to decipher the relationships between fluid and gold deposition when gold particles are not directly observed with fluid inclusions (Klein 1998; Klein et al., 2000). Another important tool to discuss conditions of precious metal deposition is supplied by stable isotopes.

Here, we present the first microthermometric measurements obtained on fluid inclusions in quartz (Ali Addé and Hes Daba sites) and (C, O) stable isotope study of ores from hydrothermal veins (Arta, Hes Daba and Asa Leyta sites), hosted by synrift volcanic rocks ranging in age from 18 to 1 Ma. These results are discussed in terms of fluid history in relation to mineralization.

The aim of our study is to investigate the relationships between fluid inclusions, and mineral textures associated with major Au-Ag-bearing veins. C and O isotopes in calcite veins and secondary calcite associated to quartz veins are also studied. We also elaborate the first geological maps of gold deposits based on gold results reported in Moussa et al., 2012 in these different synrift volcanic sites.The results are used to discuss gold behavior in fluids and precipitation processes of the Asal rift fossil geothermal system.

2. Geological setting and mineralogy

2.1 The Ali Addé site

The Ali Addé hydrothermal site is located in 15-11 Ma-old Mablas felsic series exposed on the NE flank of the Ali Sabieh antiform (Fig. 1B) (Gadalia, 1980; Le Gall et al., 2010). The Mablas series is dominated by volcanics, including rhyolitic lavas and ignimbrites, and their related feeder dyke swarms, in addition to subordinate mafic effusive products (Fig. 2A) (Gasse et al., 1986). The submeridian and 100 m-long studied cross-section shows a 30 m-wide acidic intrusion cutting through highly altered mafic volcanics. The central part of the intrusion is dissected by a steeply-dipping faulted zone, about 10 m-wide and trending N80° (Fig. 2B). Hydrothermal products are dominated by a silica-rich stockwork that comprises two types of veins: (1) chalcedony veins enriched with sulfides such as chalcopyrite, pyrite, pyrrhotite, sphalerite, galena, digenite, marcasite (Fig. 3), in addition to disseminated adularia, and (2) younger quartz barren of sulfides (Fig. 2C). Secondary minerals consist of bornite, digenite, covellite, marcasite, chalcocite and goethite. Alteration minerals such as illite and chlorite are also present. Minor minerals such as native Te, hessite and tetradymite; associated to chalcedony veins have also been identified (Figs. 2D-E; Fig. 3).

2.2 The Arta site

The Arta hydrothermal site occurs in a submeridian anticlinal structure, ca 10 km-wide, cored by 9-4 Ma-old Dalha basalts, and flanked to the east by downthrown Gulf basalts in the Djibouti plain, and to the west by Stratoid series basalts flooring the Afar depression (Fig. 1B). To the north, the Arta anticline intersects at high angle the Tadjoura gulf axis, and provoked the blockageand offset of the rift propagation into the Ghoubbet trough (Fig. 1B) (Daoud et al., 2011). In the deeply eroded core of the Arta antiform, felsic lavas of the 4-3 Ma Ribta formation overlie unconformably the tilted Dalha basalts. These volcanics are intensely cut by a dense network of submeridian fault/fractures, parallel to Ribta feeder dykes, that

display both extensional and strike-slip displacements (Robineau 1979). The Arta mineralized site is located in the crestal zone of the antiform, in the vicinity of the Stratoid unconformity. Hydrothermal veins preferentially occur within a narrow brecciated zone that extends over ca 2 km, parallel to vertical and submeridian Ribta felsic dykes (Fig. 4A). Vein orientations are in the range N20-160°E. Veins cross-cutting relationships indicate that sinistral en echelon mineralized fractures are cut and post-dated by dextral faults devoid of any mineralization. Mineralized veins are spatially confined to felsic dyke margins, and they are filled with brecciated material, chalcedony and sulfides. Banded chalcedony, quartz and carbonate veins with spacing in the range 2-10 m, typically characterize that zone (Fig. 4B). Native gold occurrences are observed, in association with electrum, pyrite, pyrrhotite, argentite, hematite, and goethite, in chalcedony veins (Fig. 3). Two types of calcite have been identified. The first ones are associated to mineralized veins or breccias. The second types, not associated to hydrothermal mineralization, occur in the field as >20 m-long veins. The main mineralized veins (Au > 1 ppm) appear to be genetically linked to strike-slip faults (Fig. 4-A). The less enriched or barren veins correspond to carbonate- or breccia-filled veins (Fig. 4-C-D).

2.3 The Hes Daba site

The Hes Daba hydrothermal site is located between the Gaggade and Asal faulted depressions, in one of the felsic extrusions interstratified in the intermediate member of the 3.3-1 Ma-old Stratoid series basalts (Fig. 1B). The topography is surrounded by NW-SE-oriented tilted fault blocks of Stratoid series basalts. Most of mineralizations are observed in a network of > 2 km-long rift-parallel veins cutting through dominantly trachytic lavas (Moussa et al., 2012) (Fig. 5A). The highest gold concentration is controlled by fractures (Fig. 5A).

The gangue mainly comprises chalcedony ± adularia veins, massive quartz and to a lesser extent carbonate (Figs. 5B-C-D-E). Several quartz veins up to 1m thick contain disseminated

hypogene (chalcopyrite, pyrite, sphalerite, pyrrhotite, galena, hessite, petzite, electrum, argentite and hematite) and supergene minerals (bornite, digenite, covellite, chalcocite, native Cu, native Ag, native Au and marcasite) (Fig. 3). Telluride minerals are expressed as grains of hessite ($Ag_{1,98}$ $Te_{1,02}$) disseminated in quartz

Alteration minerals such as chlorite have also been identified. Late carbonate veins barren of sulfides and gold are common.

2.4 The Asa Leyta site

The Asa Leyta hydrothermal site is exposed on a 2 km-long transect cutting at high angle the Stratoid basalts series, on the western edge of the Asal rift (Fig. 1B). The oldest exposed volcanic rocks are highly fractured trachybasalt, showing a preserved pattern of vertical magmatic prisms. They are overlain by tens of m thick pile of stratified felsic lava flows, with spherulitic rhyolites at their base, which are involved into a long wavelength antiform. Locally, the irregular top surface of the pre-acidic trachybasalts is capped by a 10 m-thick sequence of undated greenish sandstones with thin gypsum layers. Gypsum is also observed as fracture-filling product in the >10 m-thick package of slightly tilted lacustrine silts occurring at the eastern extremity of the Asa Leyta section (Fig. 6A). The two gypsum-rich lacustrine sediments flanking the felsic volcano are, in turn, overlain by young basalts. They represent two gypsum ± anhydrite stockworks probably related to a paleo-Asal saline lake. Additional mineralization are evidenced as a dense and steep network of chalcedony and calcite-rich veins with a dominant N140°E trend, parallel to the Asal extensional fault system (Moussa et al., 2012) (Figs. 6B-C). Pyrite is the most common mineral. Platy calcite, usually pseudomorphed by quartz, is also present (Fig. 3). Banded chalcedony ± adularia and calcite veins are spatially associated with the trachytic lavas whereas breccias are preferentially linked to felsic intrusions. Alteration minerals such as clinochlore and albite are also present.

These samples are mainly form of carbonate ± quartz veins. Samples with gold are associated to chalcedonic ± adularia veins containing pyrite with secondary minerals (goethite and calcite). The highest value of gold corresponds to 10 ppm (Moussa et al., 2012).

3. Methodology

Polished-thin sections of rock samples from hydrothermal ore deposits were examined with a reflected-transmitted light microscope at magnification up to 1000 in dry air and oil immersion objectives. Additional analyses were performed by using: i) X-Ray diffraction (XRD) analyses to determine major minerals in gangue and alteration zones in powder samples and ii) X-ray elemental mapping by using CAMECA SX100 electron-microprobe with PAP correction program (Pouchou and Pichoir, 1984). To search telluride minerals, operating conditions consisted in accelerating voltage of 25 KV, beam current at 20 nA and beam size at 1 μm^2. This work has been conducted at Laboratoire de Géochimie et Métallogénie, IFREMER, Brest.

Primary, pseudo-secondary and secondary inclusions were distinguished using criteria summarized by Roedder (1984). Primary fluid inclusions occur in well-defined growth zones. Double polished thin sections of more than 50 samples were prepared at the Laboratory of Géochimie et Métallogénie, IFREMER (Brest, France). These are vein samples from the Ali Addé and Hes Daba sites. Only 8 samples were suitable for fluid inclusion studies. Fluid inclusions were studied in secondary quartz veins. Primary fluid inclusions occur in well-defined growth zones. Microthermometric measurements were performed using Linkam platinum gas heating and freezing stage and Raman spectrometry located at the GeoRessources Laboratory in Nancy (France). The data are reproducible to ±3°C for heating runs and ±0.1°C for freezing runs.

In addition, oxygen and carbon isotopes of calcite veins from three hydrothermal sites

commonly regarded as the more mineralized areas (Hes Daba, Arta, Asa Leyta) have been analyzed at Royal Holloway University of London (UK) following standard methodology of McCrea (1950). Isotopic ratios are reported in per mil (‰) relative to the international standard of V-SMOW (Vienna Standard Mean Ocean Water) for oxygen and PDB (Pee Dee Belemnite) for carbon using the conventional δ-notation. Samples and standards were run in duplicate. Results were standardized based on six internal carbonate standards that were calibrated using international standards NBS-19. The analytical precisions based on weighting are ± 0.03‰.

3.1 Quartz and calcite textures

Quartz is the most common hydrothermal mineral in veins. A wide range of grain sizes and morphologies giving rise to several textures typical of low-sulfidation epithermal deposits have been observed in the Ali Addé, Hes Daba and Arta mineralized sites. The most common textures observed in our samples are: i) microcrystalline quartz (Fig. **7**A), ii) plumose quartz texture (Fig. **7**B), iii) crustiform and colloform banded texture quartz (Figs. **7**C), iv) jigsaw textured quartz (Figs. **7** D, G-H), and finally v) massive and bladed calcite from Arta, Hes Daba and Ali Addé sites. The massive calcite is not associated with mineralization.

4. Results

4.1. Microthermometric data

The microthermometric measurements are summarized in Fig. 8. The fluid inclusions have a variety of irregular shapes. Two types are observed and the most common are two-phase liquid-rich inclusions, containing approximately 90% liquid and 10% vapor, they homogenize to a liquid phase upon heating. Vapor-rich inclusions are less common, the amounts of liquid

in these inclusions are very low (< 5%), and the homogenization temperature (Th) values have not been determined. Other transition phase changes have not been observed (e.g. minerals; clathrates melting or CO_2 liquid vapor homogenization). Fluid inclusions from the Ali Addé site display size less than 20 μm. Th in all the veins and homogenization temperature ranges from 150° to 283°C. Ice melting temperatures (Tm) range between -0.2°C to - 1.6°C indicating that inclusion solutions contain 0.2 to 2.7 eq. wt % NaCl (Bodnar, 1992).

In the Hes Daba site, two types of fluid inclusion assemblages show different temperatures. The first inclusion type, observed in barren veins (60 ppb on gold), have a Th ranging from ~180 to 300°C. Ice melting temperatures are between -0.2° and -4.4°C indicating that salinity is comprised between 0.35 and 7 eq. wt % NaCl. The second type of fluid inclusions are in quartz associated with gold and exhibit homogenization temperature (Th) ranging from 190 to 340°Cwith most of the data between 230 to 250°C. Ice melting temperatures range between -0.2 and -2°C indicating that inclusions contain 0.7 to 3.4 eq. wt % NaCl respectively.

4.2. C and O stable isotopes

The $\delta^{13}C$ values of calcite from the Asa Leyta site range from -4.6 to 0.3‰ while $\delta^{18}O$ values vary between 5 and 17.5‰ (Tab. 1). The Hes Daba hydrothermal site is characterized by $\delta^{13}C$ and $\delta^{18}O$ isotope compositions of carbonate veins that cluster between -5.8 to -2.7‰ and 8.2 to 18.7‰, respectively. Mineralized veins from the Arta site have $\delta^{13}C$ composition of calcite between -7.5 to -1.1‰ while the $\delta^{18}O$ values span between 3.7 to 26.6‰. Calcite veins occur in more than 20 m high and extend over distances of ~ 10 m in Asa Leyta, Arta and Hes Daba (Fig. 4D, 5D-E, 6C).

5. Discussion

5.1. Fluid inclusions

The Th and Tm values observed at Hes Daba and Ali Addé sites are consistent with temperatures and salinities commonly described for precious metal-bearing epithermal deposits and active geothermal systems (e.g. Bodnar et al., 1985; Hedenquist and Henley 1985 a, b, Heald et al., 1987; Simeone and Simmons, 1999; Wilkinson, 2001). The low salinity of the solutions and the absence of CO_2 and minerals (halite, sylvite) suggest that the main component was meteoric water (Head et al., 1987). In addition, there is also fluid inclusion with salinities of 7 eq. wt % NaCl equiv. This relatively high salinity could be explained by the mixing of two fluids with different salinities or by phase separation as suggested elsewhere by Simmons and Brown (1997). Phase separation is classically considered to explain low and high salinity fluids on deep-sea Mid Ocean Ridges (Von Damm et al., 1997). If we consider that our fluid originated from magmatic fluids and rich in CO_2; it can undergo under: i) phase separation and produce low salinity fluids but in this case the vapor phase should be enriched in CO_2 or ii) hydrothermal fluid resulting from the interaction between seawater and volcanic rocks having also phase separation but this implies that the vapor phase will not be enriched in CO_2 and iii) meteoric fluids but the absence of chlorine does not made easy the transport of metals.

On the other hand, the observed variations of the Tm values at Hes Daba could also be consistent with the presence of small amounts (not detected) of dissolved CO_2 and with the multi-stage nature of the veins. This could also suggest depressurization of fluid with phase separation and precipitation of metals in relation with tectonic activities. In fact, the multi-stage evolution of the mineralized veins as evidenced by their banded and brecciated structures, indicate episodic introduction of the hydrothermal fluids over the life of the system. In fact, the existence of multiple quartz textures may represent successive quartz

generations. Much of the observed textures are characterized by: i) aggregates of microcrystalline texture, ii) jigsaw quartz textures, iii) colloform with a plumose texture. These textures are characteristic of epithermal system (Moncada et al., 2012) and indicate multiple episodes of fluid circulation along the rift faults system; and iv) both, bladed and massive calcites are observed in our samples. The bladed calcite has been reported as an indicator of boiling solution (Mayer et al., 2002; Simmons et al., 2005). Dong and Zhou (1996) suggested that massive calcite is late and not associated with mineralization in the Cracow epithermal vein system, Australia. Similarly, massive calcite is not associated to mineralization in the hydrothermal sites under study here and support that phase separation played an important role in the genesis of mineralization. In addition, the Th *versus* Tm diagram indicates a wide range of values for ore-bearing fluids from a solution of high to low temperatures for both sites (Fig. 9). The Th variations suggest that these veins were formed by several pulses of solutions at different temperatures. This suggestion is also supported by the various types of textures in the veins and the breccias.

The higher Th values obtained in both sites associated with sulfide minerals (Hes Daba and Ali Addé) suggest a deposition of sulfide at high temperature. This indicate that in Hes Daba and Ali Addé the sulfide and gold assemblage comprising chalcopyrite, pyrite, sphalerite, galena, bornite, digenite, marcasite, and hematite formed at temperature close to 250°C. Furthermore, samples with high Tm values (-4.4°C) in the Hes Daba site are devoid of any sulfide or precious metal and minerals.

In addition, the occurrence of adularia and illite indicate that the pH of these solutions was near neutral. On the other hand, the presence of Te at Ali Addé and Hes Daba sites suggests temperature conditions <300°C for the hydrothermal fluid (Afifi et al., 1988; Tooth et al., 2008).

In the Djibouti rift system, boiling conditions are also recorded by the presence of platy calcite, banded texture and high concentration of As (Moussa et al., 2012). Seward (1973) and Giggenbach (1997) suggested that the occurrence of pyrite with chlorite indicates that gold-silver are transported as bisulfide complexes in hydrothermal solutions. In our hydrothermal sites, pyrite and chlorite have been described at Ali Addé and Hes Daba sites. Therefore, it is here suggested that gold could have been transported as bisulfide complexes in Hes Daba and Ali Addé areas although multiple sources of fluids are documented in these sites (Moussa et al., 2017). Furthermore; Moussa et al., 2012 reported two different stages of hydrothermal ore deposits: i) the first stage corresponds to massive quartz –containing sulfide minerals; ii) the second stage is characterized by the formation of chalcedony gangue containing gold and sulfide minerals. Chalcedony is classically reported to form at shallow depth at temperature between 190 to 100°C (Sander and Black, 1988; White and Hedenquist, 1990). In this study, we have evidence that the first stage occurred in a high temperature hydrothermal (180 to 340°C) system with sulfide minerals (chalcopyrite, sphalerite, galena, pyrrhotite, tetradymite, hematite and magnetite) and the second stage associated to chalcedony±adularia veins in shallow depth. This stage is characterized by the deposition of gold and electrum.

5.2 . Behavior of gold in the Asal rift system

The Asal rift in Djibouti is the locus of active hydrothermal discharge (carbonate chimneys, hot springs and fumaroles). Drilled geothermal wells in the Asal area display temperatures up to 350°C at depths of 2105 m (D'Armore et al., 1998). The classical mineral zonation commonly observed in geothermal systems (Henley and Ellis 1983; Hedenquist et al., 2000; Simmons and Browne 2000) has also been identified in the Asal geothermal field. This zonation consists of (i) unweathered basalts from surface to 250 m depth, (ii) a smectite zone (depth between ~250 and 600 m); (iii) a silicate zone (260 to 280°C) with epidote, prehnite, feldspars, pyrite, chlorite, pyroxenes and garnet (depth between 850 and ~1,300 m), and (iv) a

Ca-silicate zone characterized by amphibole, clinopyroxene and garnet (depth of ~2,013 m) (D'Armore et al., 1998). Sulfide minerals were also found at about 850 m depth (D'Armore et al., 1998).

In this section, we calculated the distribution of aqueous species at reservoir conditions using two software packages, Phreeqc 3.0 (Parkhurst and Appelo, 2015) and Geochemist's Workbench 10 (Bethke and Yeakel, 2008). The program Phreeqc was used to calculate the activities of species of the reservoir fluid compositions from analytical data of fluid and gold reported in D'Armore et al. (1998) and Simmons et al. (2016), respectively. The data used here are from the Asal geothermal field and all the aqueous metal concentrations come from analyses of downhole samples (Table 1) (D'Armore et al., 1998). As suggested by Simmons et al. (2016) about many geothermal systems (Broadland-Ohaaki, Rotokawa and Waiotapu, New Zealand), gold and silver depositions likely occur in production wells, hot springs and reservoir rocks. The most important ligands in hydrothermal gold-bearing solutions are chloride and reduced sulfur (Henley, 1985; Gibert et al., 1998). In near neutral epithermal systems, the loss of H_2S during boiling conditions results in the high fugacity of S^{2-} and HS^- in the solution which in turn leads to the transport of gold as bisulfide complexes (reaction 1) (Henley, 1985). In this type of solution, the transport of gold is independent of the activity of Cl^-. However, if salinity increases and pH decreases, gold is transported by chloride complexes (reaction 2) and other base metals can be associated, following the equations (Seward, 1989).

$$Au^+ + H_2S + HS^- = Au(HS)^-_2 + 0.5H_2 \quad (1)$$

$$Au^+ + H^+ + 2Cl^- = AuCl_2^- + 0.5H_2 \quad (2)$$

Here, we modeled the precipitation of gold using a plot for the fugacity of oxygen *versus* pH. Diagram 1 shows that elemental gold is more stable with increasing pH and decreasing O_2

fugacity (Fig. 10). At low pH and high fugacity, gold is in solution species as $AuCl_2^-$. On the other hand, the fluid and mineralogy compositions of the Asal geothermal system and all the springs have been investigated from isotopic and geochemical approaches (Fouillac et al., 1989; D'Armore et al., 1998; San Juan et al., 1990). All these studies concluded that there was a mixing between magmatic, meteoric and seawater fluids.

5.3 . Origine of calcite

The values of C and O isotope compositions in carbonate are illustrated in Table 2. These carbone and oxygen values for the three sites (-7.5 to -0.3‰ for $\delta^{13}C$ and 3.7 to 26.6‰ for $\delta^{18}O$) are consistent with values found in epithermal and geothermal deposits elsewhere (e.g. -10 to 1‰; Ohmoto and Rye, 1979; Bethe and Rye, 1979; Field and Fifarek, 1985). The data plot of calcite ^{13}C *versus* calcite ^{18}O values are presented in Fig. 11. The $\delta^{13}C$ value of magmatic carbon is between -7 and -2‰ (Ohmoto and Rye, 1979; Deines et al., 1991; Cartigny et al., 1998). The $\delta^{18}O$ values of magmatic fluids are between 5.5 and 9‰ (Taylor, 1974a, 1979). Therefore, we can suggest that at Hes Daba and Asa Leyta sites, both ^{13}C and ^{18}O values typically characterize fluids with deep origin water and the possibility of cooling process. The low ^{18}O values of all sites (Hes Daba, Arta and Asa Leyta) could be explained by the contribution of meteoric water interacting with marine seawater for Asa Leyta (Fig. 11). Calcites from Gold Cross area (New Zealand) show value of oxygen isotope compositions (3.8 and 15.4‰) which suggest that the calcites originated from a CO_2-rich vapor phase (Simmons et al. 2000). Other examples of calcite indicating boiling conditions are documented elsewhere, as in the Waiotapu geothermal area, New Zealand (Hedenquist and Browne, 1989; Simmons and Christenson, 1994).

In Djibouti, it has been argued from two deep geothermal boreholes drilled in the Asal rift, that oxygen isotope compositions range from +4.6 to 12.2‰ for whole-rock samples, from

+7.3 to + 14.3‰ for newly-formed quartz and from +7.8 to 20.4‰ for newly-formed calcite (Fouillac et al., 1989). These authors concluded that $\delta^{18}O_{mineral}$ – values tend to decrease with depth, whilst data on the newly-formed quartz allow reliable reconstruction of the thermal log, indicating a zone where fluid circulation occurred at higher temperatures, with probable influx of deep CO_2.

Therefore, we suggest that calcite from Hes Daba, Arta and Asa Leyta sites originated from phase separation of liquid and gas involving exsolution of carbon dioxide and steam formation (e.g. boiling). In fact, as assessed by Dong et al. (1990), in the case a fluid undergoing boiling that result in the loss of CO_2 without rapid cooling, calcite could precipitate alone or is later replaced by silica minerals forming for example lattice-bladed textures. These types of textures have been identified at Hes Daba, Arta and Asa Leyta sites, hence confirming again that those sites underwent several phases of phase separation and probably silica mineral deposits.

Based on field and mineralogical observations, Moussa et al. (2012) identified different types of mineralization that they related to various depths in the SE Afar hydrothermal rift system. Apart from the deepest zone which recorded epidote alteration in the Ali Sabieh antiformal area, as well as in the Asal rift, two different structural depths have been identified as i) relatively deep levels with massive quartz veins containing sulfides (Hes Daba, Ali Addé and Arta sites) and brecciated veins (Da'asbiyo, Babba Alou and Asa Leyta), and ii) shallow structural levels with evidence of boiling conditions where chalcedony with adularia and platy calcite are common (Ali Addé, Hes Daba, Arta and Asa Leyta sites). Gold is mostly concentrated in the latter type whereas massive quartz or breccias are less enriched or barren (Figs. 4-5). In addition, Moussa et al. (2017) identified the source of mineralization with sulfur and strontium isotopes and they further suggested that two major types of fluids contributing to the formation of ore deposits were i) hydrothermal fluids enriched in

magmatic volatiles and leading to significant leaching of the underlying volcanic rocks (Da'asbiyo, Ali Addé, Hes Daba, Arta and Babba Alou sites) and ii) hydrothermal fluids probably initially enriched in magmatic SO_2, but that underwent significant dilution with seawater and/or contamination with evaporite layers that later dissolved during the circulation of the hydrothermal fluids (e.g. Babba Alou, Arta Plage and Asa Leyta sites).

In this work, we have investigated the fluid inclusions (Ali Addé and Hes Daba) and stable isotopes (Arta, Hes Daba and Asa Leyta) of the most mineralized sites. Based on these results, we suggest that three types of hydrothermal fluids, instead of two, hydrothermal fluids; have contributed to the formation of ore deposits in Djibouti, e.g. i) those enriched in magmatic volatiles with probable interaction with volcanics rocks (Ali Addé and Hes Daba), ii) those enriched in magmatic volatiles diluted by meteoric water (Ali Addé, Hes Daba and Arta), and iii) those enriched in magmatic SO_2 that underwent significant dilution with seawater and/or contamination with evaporite layers (Asa Leyta). In addition, previous authors demonstrated the importance of saline, magmatic and meteoric water in the geothermal system of the Asal rift (Sanjuan et al., 1990; Fouillac et al., 1998). In the previous section, it has been stated that at low pH and high fugacity (O), gold is expressed as $AuCl_2^-$, while being more stable with high pH. This suggests that magmatic fluid probably has been diluted. Given the specific location of the Hes Daba and Asa Leyta sites on the western edge of the Asal rift trough (Fig.12), it can be confidently assessed that mineralization, even when associated to late felsic intrusions, might have recorded in the past the composition of the Asal fluid (e.g. magmatic, meteoric and saline). In that case, it will be important to investigate inclusions enclosed in newly-acquired samples from drill cores and collected samples in the Asal rift axis in order to find supportive evidence for magmatic fluids and saline waters.

Therefore, three different types of hydrothermal systems could be recognized in this part of the SE Afar rift as: i) fossil submarine ones (Asa Leyta); 2) fossil hydrothermal with meteoric water (Ali Addé, Hes Daba and Arta) and 3) the active geothermal system (Asal rift).

6. Conclusions

The range of Th values is consistent with an epithermal environment. This study suggest that in Djibouti rift system, low sulfidation epithermal system with generally low salinity fluids has been identified, although relatively high salinity fluids existed. The stable isotope signature of the ore forming fluid suggest contributions of both meteoric and magmatic fluids with a mixing process with probably different proportion between both types of fluids possibly related to mineralization, although seawater fluids are suspected from the lowest values of $\delta^{18}O$ for Asa Leyta site. This suggestion is also supported by the S and Sr stable isotopic signature from mineralized veins (Moussa et al., 2017). Gold is related to pyrite occurring either in chalcedony veins within fractures. The main mechanism for gold deposit was boiling as indicated by evidence like the occurrence of quartz textures, adularia, platy calcite and mineral textures. Combining fluid inclusion and stable isotopes could be used to predict the potential of hydrothermal veins during drilling and exploration in the Djibouti active and fossil rift system.

Futhermore, in July 2018 a survey of the Fialé geothermal field of the Asal Rift system started. We suggest that the concentration of gold must be analyzed and estimated as it is done in other countries in the world with a high geothermal potential (New Zealand). The high salinity found in this region is favorable for the concentration and transport of metals (e.g., Au, Cu, Ag…) and rare elements. Therefore, our goal has to be to develop a method to extract, analyze and understand the behavior of those elements in the future that will represent a unique good opportunity for this small country both scientifically and economically.

Acknowledgments

This research has been supported by the CERD (Center for Research and Studies of Djibouti) and the SCAC (Service de Cooperation et d'Action Culturelle Français). We are warmly grateful to Dr A.M. Caminiti for his help in the field and to Dr Jalludin Mohamed for all his support during this research. We are also grateful to M. Bohn for his help and assistance for electron microprobe analyses. We would like to thank the Centre National d'Etudes Spatiales (CNES) for their support for providing us the SPOT 5 satellite images. We would like to thank Dr B. Cavalazi; Prof. Y. Morishita and the handling editor Prof. F. Pirajno for their constructive comments that greatly improved the manuscript.

References

Afifi A, Kelly W, Essene E., 1988. Phase relations among tellurides, sulfides, and oxides; I, Thermochemical data and calculated equilibria. Econ. Geol., 83: 377.

Andre-Mayer, A.S., Leroy, J.L., Bailly, L., Chauvet, A., Marcoux, E., Grancea, L., Llosa, F., Rosas, J., 2002. Boiling and vertical mineralization zoning; a case study from the Apacheta low-sulfidation epithermal gold-silver deposit, southern Peru. Mineral. Deposita, 37(5), 452-464.

Audin L., Quidelleur X., Coulié E., Courtillot V., Gilder S., Manighetti I., Gillot P.Y., Tapponnier P., Kidane T., 2004. Paleomagnetism and K-Ar and 40Ar/39Ar ages in the Ali Sabieh area (Republic of Djibouti and Ethiopia): constraints on the mechanism of Aden ridge propagation into southeastern Afar during the last 10 Myr. Geophys. J. Int., 158, 327-345.

Barberi, F., Ferrara, G., Santacroce, R. Varet, J., 1975. Structural evolution of the Afar triple junction Afar Depression of Ethiopia: Stuttgart, Germany, Schweizerbart, Scientific Report, 14, 38-54.

Barton, P.B., Bethke, P.M., Roedder, E., 1977. Environment of ore deposition in the Creede mining district, San Juan Mountains, Colorado; Part III, Progress toward interpretation of the chemistry of the ore-forming fluid for the OH Vein. Econ. geol., 72(1), 1-24.

Bethke, C.M., Yeakel, S., 2008. The Geochemist's Workbench® - Release 7. GWB Essentials Guide. Hydrogeology Program. University of Illinois, 489 pp.

Bodnar, R.J., Reynolds, T.J., Kuehn, C.A., 1985. Fluid-inclusion systematics in epithermal systems. Rev. Econ. Geol., 2, 73-97.

Bodnar, R.J., 1992. Contributions of fluid inclusion studies to gold deposit research. In: International Symposium on Fluid Inclusions in Gold Deposit Research and Prospecting, Beijing, Abstracts & Program, l-2.

Bodnar, R.J., Reynolds, T.J., Kuehn, C.A., 1985, Fluid inclusion systematics in epithermal systems. In Berger, B.R., Bethke, P.M., eds., Geology and Geochemistry of Epithermal Systems. Rev. Econ. Geol., 73-97.

Bodnar R.J., 1993. Revised equation and table for determining the freezing point depression of H_2O-NaCl solutions. Geochim. Cosmochim. Acta, 57, 683-684.

Boiron M.C., Cathelineau M., Ruggieri G., Jeanningros A., Gianelli G., Banks D., 2007. Active contact metamorphism and CO_2-CH_4 fluid production in the Larderello geothermal field (Italy): the fluid inclusion data. Chem. Geol., 237, 303-328.

Brown, K.L., 1989, Kinetics of gold precipitation from experimental hydrogen sulfide solutions. Econ. Geol., 6, 320-327.

Browne, P.R.L. Ellis, A.J., 1970. The Ohaki- Broadlands hydrothermal area, New Zealand: Mineralogy and related geochemistry. Amer. J. Sci., 269, 97-131.

Cartigny P., Harris J.W., Javoy M., 1998. Eclogitic diamond formation at Jwaneng. No room for a recycled component. Science, 280, 1421-1424.

Ciobanu C., Cook N., Pring A., 2005. Bismuth tellurides as gold scavengers. In: Mineral Deposit Research: Meeting the Global Challenge. Springer, Berlin, Heidelberg1383-1386.

Cook N., Ciobanu C., 2005. Tellurides in Au deposits: implications for modelling. In: Mineral Deposit Research: Meeting the Global Challenge. Springer, Berlin, Heidelberg, 1387-1390.

Coplen, T.B., Kendall, C., Hopple, J., 1983. Comparison of stable isotope reference samples. Nature. 236-238.

Daoud, M.A., Le Gall, B., Maury, R.C., Rolet, J. Huchon, P. Guillou, H., 2011. Young rift kinematics in the Tadjoura rift, western Gulf of Aden, Republic of Djibouti. Tectonics, 30, doi.org/10/1029/2009TC002614.

Deines P., Harris J.W., Gurney J.J., 1991. The carbon isotopic composition and nitrogen content of lithospheric and asthenospheric diamonds from the Jagersfontein and Koffiefontein kimberlite, South Africa. Geochim. Cosmochim. Acta, 55, 2615-2625.

Dong, G., Zhou, 1996. Zoning in the Carboniferous-Lower Permian Cracow epithermal vein system, central Queensland, Australia. Mineral. Deposita, 30 (1), 210-224.

Dong, G., Morrison, G., Jaireth, S., 1995. Quartz textures in epithermal veins, Queensland; classification, origin and implication. Econom. Geol., 90 (6), 1841-1856.

Doubre C., Manighetti I., Dorbath C., Louis. D., Jacques E., Delmond J.C., 2007. Crustal structure and magmato-tectonic processes in an active rift (Asal-Ghoubbet, Afar, East Africa): 1. Insights from a 5 month seismological experiment. J. Geophys. Res. Solid Earth. 112 (B5), 1-32.

Douville E., Charlou J.L., Donval J.P., Hureau D., Appriou P. 1999. Le comportement de l'arsenic (As) et de l'antimoine (Sb) dans les fluides provenant de différents systèmes hydrothermaux océaniques. C. R. Acad. Sci. Paris, 328, 97-104.

Gadalia, A., 1980. Les rhyolites du stade initial de l'ouverture d'un rift : Exemple des rhyolites miocènes de l'Afar. Thesis, University of Orsay.

Gasse F., Dagain J., Mazet G., Richard O., Fournier M., 1986. Carte géologique 1 :100 000 de la République de Djibouti: feuille de Dikhil, Ministère Français.

Giggenbach, W.F., 1997. The origin and evolution of fluids in magmatic-hydrothermal systems. Geochem. Hydrothermal. Ore Deposits, 3, 737-796

Field, C.W., Fifarek, R.H., 1985. Light stable isotope systematic in epithermal systems. Rev. Econ. Geol. 2, 99-128.

Fouillac, A., Fouillac, C., Cesbron, F., Pillard, F., Legendre, O., 1989. Water-rock interaction between basalt and high-salinity fluids in the Asal Rift, Republic of Djibouti. Chem. Geol., 76, 271-28.

Fournier, R.O., 1985. The behavior of silica in hydrothermal solutions. Rev. Econ. Geol., 2, 45-61.Klein, E.L., 2000 Fluid inclusion studies on Caxias and Areal gold mineralizations, Sao Luis Craton, northern Brazil . J. Chem. Explor., 71, 51-72.

Kokh, M.A., Lopez, M., Gisquet, P., Lanzanova, A., Candaudap, F., Besson, P., Pokrovski, G.S., 2016. Combined effect of carbon dioxide and sulfur on vapor–liquid partitioning of metals in hydrothermal systems. Geochim. Cosmochim. Acta, 187, 311-333.

Haas, J.L., 1971. The effect of salinity on the maximum thermal gradient of a hydrothermal system at hydrostatic pressure. Econ. Geol. 66, 940-946.

Hagemann, S.G., Brown, P.E., 1996. Geobarometry in Archean lode-gold deposits. Eur. J. Mineral., 8, 937-960.

Heald, P., Foley, N.K., Hayba, D.O., 1987. Comparative anatomy of volcanic-hosted epithermal deposits; acid-sulfate and adularia-sericite types. Econ. Geol., 82(1), 1-26.

Hedenquist, J.W., Browne, P.R., 1989. The evolution of the Waiotapu geothermal system, New Zealand, based on the chemical and isotopic composition of its fluids, minerals and rocks. Geochim. Cosmochim. Acta, 53(9), 2235-2257.

Hedenquist, J.W., Arribas, R.A., Gonzalez-Urien, E., 2000. Exploration for epithermal gold deposits. Rev. Econ. Geol., 13, 245-277.

Hedenquist, J.W., Henley, R.W., 1985a. Hydrothermal eruptions in the Waiotapu geothermal system, New Zealand. Econ. Geol., 80, 1640-1668.

Hedenquist, J.W., Henley, R.W., 1985b. The importance of CO2 on freezing point measurements of fluid inclusions: Evidence from active geothermal systems and implications for epithermal ore deposition. Econ. Geol., 80, 1379-1406.

Henley, R.W., Hughes, G.O., 2000. Underground fumaroles: “Excess heat” effects in vein formation. Econ. Geol., 95(3), 453-466.

Henley, R.W., 1985. The geothermal framework of epithermal deposits. In: Berger, B.R. and Bethke, P.M. (eds) Geology and geochemistry of epithermal systems. Rev. Econ. Geol. 2, 1-24.

Le Gall, B.., Daoud, M.A., Maury, R.C., Rolet, J., Guillou, H., Sue, C., 2010. Magma-driven antiform structures in the Afar rift: the Ali Sabieh range, Djibouti. J. Struct. Geol., 32, 843-854.

Manighetti, I., Tapponnier, P., Courtillot, V., Gruszow, S., 1997. Propagation of rifting along

the Arabia-Somalia plate boundary: the gulfs of Aden and Tadjoura. J. Geophys. Res., 102, 2681-2710.

Marcoux E, Moelo Y, Leistel J.M., 1996. Bismuth and cobalt minerals as indicators of stringer zones to massive sulphide deposits, Iberian Pyrite Belt. Mineralium Deposita, 31, 1-26.

Mavrogenes J.A., R.J. Bodnar, J.R. Graney, KG. McQueen, K. Burlinson, 1995. Comparison of decrepitation, microthermometric and compositional characteristics of fluid inclusions in barren and auriferous mesothermal quartz veins of the Cowra Creek Gold District, New South Wales, Australia. J. Geochemi. Explor. 54, 167-l75.

McCrea J.M., 1950. On the isotopic chemistry of carbonates and a paleotemperature scale. J. Chem. Phys., 18, 849-857.

Moncada, D., Mutchler, S., Nieto, A., Reynolds, T. J., Rimstidt, J. D., Bodnar, R.J., 2012. Mineral textures and fluid inclusion petrography of the epithermal Ag–Au deposits at Guanajuato, Mexico: Application to exploration. J. Geochem. Explor, 114, 20-35.

Moussa, N., Rouxel, O., Grassineau, N.V., Ponzevera, E., Nonnotte, P., Fouquet, Y., Le Gall, B., 2017. Sulfur and strontium isotopic study of epithermal mineralization: a case study from the SE Afar Rift, Djibouti. Ore Geol. Rev., 81, 358-368.

Moussa, N., Fouquet, Y., Le Gall, B., Caminiti, A. M., Rolet, J., Bohn, M., Jalludin, M., 2012. First evidence of epithermal gold occurrences in the SE Afar Rift, Republic of Djibouti. Miner. Deposita, 47, 563-576.

Ohmoto, H., Rye, R.O., 1979. Isotopes of sulfur and carbon. In: Barnes, H.L. (Ed.), Geochemistry of Hydrothermal Ore Deposits, 2nd ed. Wiley, New York. 509-567.

Parkhurst, P., Appelo, D.L., 2015. Description of Input and Examples for PHREEQC Version 3–A Computer Program for Speciation, Batch-Reaction, One-Dimensional Transport, and Inverse Geochemical Calculations (http://wwwbrr.cr.usgs.gov/projects/GWC_coupled/phreeqci/)

Pouchou L., J, Pichoir, F., 1984. New model quantitative x-ray microanalysis. Application to the analysis of homogeneous samples. Recherche Aerospatiale, 3, 13-38

Potty, B., Leroy, J., Jachimowicz, L., 1976. Un nouvel appareil pour la mesure des temperatures sous le microscope, l'installation de microthermométrie Chaix-Meca. Bull. Soc. Fr. Mineral. Cristallogr., 99, 182-186.

Robineau, B., 1979. La zone d'Arta et le Rift d'Asal-Ghoubbet: leur étude intégrée dans le contexte géodynamique de l'Afar. Thesis. Université des Sciences et Techniques du Languedoc. Académie de Montpellier.

Roedder, E., 1984. Fluid inclusions, 12, 12-45. P.H. Ribbe (Ed.), Washington DC, Mineral. Soc. Am.

Roedder E., Bodnar R.J., 1980. Geologic pressure determinations from fluid inclusions studies. Ann. Rev. Earth Planet. Sci., 8, 263-301.

Reyes A.G., 1990. Petrology of Philippine geothermal systems and the application of alteration mineralogy to their assessment. J. Volcanol. Geotherm. Res., 43, 279-309.

Ruggieri G., Cathelineau M., Boiron M.C., Marignac C., 1999. Boiling and fluid mixing in the chlorite zone of the Larderello geothermal system. Chem. Geol, 154, 237-256.

Samson, I., Anderson, A., Marshall, D.D. (Eds.). 2003. Fluid inclusions: analysis and interpretation, 32, Mineral. Assoc. Canada.

Sanjuan, B.,Michard, G., Michard, A., 1990. Origine des substances dissoutes dans les eaux des sources thermales et des forages de la région Asal-Ghoubbet (République de Djibouti). J. Volcanol. Geotherm. Res. 43 (1), 333-352.

Saunders, J.A., 1990. Colloidal transport of gold and silica in epithermal precious-metal systems: Evidence from the Sleeper deposit, Nevada. Geology, 18 (8), 757-760.

Saunders, J.A., 1994. Silica and gold textures in bonanza ores of the Sleeper deposit, Humboldt County, Nevada. Evidence for colloids and implications for epithermalore-forming processes. Econ. Geol., 89 (3), 628-638.

Seward, T.M. 1989. The hydrothermal chemistry of gold and its implications for ore formation: boiling and conductive cooling as examples. Econ. Geol. Monograph. 6, 398-404.

Shenberger, D., Barnes, H.L., 1989. Solubility of gold in aqueous sulfide solutions from 150 to 350°C. Geochim. Cosmochim. Acta, 53(2), 269-278.

Shepherd, T.J, Rankin A, H., Alderton D.H. 1985. Fluids inclusion in minerals: methods and applications. Virginia Tech, Blacksburg, USA.

Simmons S.F., Brown K.L., Browne R.L., Rowland J.V., 2016. Gold and silver resources in Taupo Volcanic Zone geothermal systems. Geotherm 59, 205-214

Simmons S.F., Christenson B.W., 1994. Origins of calcite in a boiling geothermal system. Amer. J. Scienc., 294, 361.

Simmons, S.F., Browne, P.R.L., 2000. Hydrothermal minerals and precious metals in the Broadlands-Ohaaki geothermal system: Implications for understanding low-sulfidation epithermal environments. Econ. Geol., 95 (5), 971-999.

Simeone, R., Simmons, S.F., 1999. Mineralogical and fluid inclusion studies of low-sulfidation epithermal veins at Osilo (Sardinia), Italy. Miner. Deposita, 34(7), 705-717.

Stietljes L., 1973. L'axe tectono-volcanique d'Asal (Afar central- Territoire français des Afars et des Issas).Thesis, Université de Paris-Sud, Orsay.

Taylor, H.P., 1974. The application of oxygen and hydrogen isotope studies to problems of hydrothermal alteration and ore deposition. Econ. Geol., 69, 843-883.

Taylor, H.P., 1997. Oxygen and hydrogen isotope relationships in hydrothermal mineral deposits. Geochemi. Hydrothermal. Ore Deposits, 3, 229-302.

Tooth B., Brugger J., Ciobanu C., Liu W., 2008. Modeling of gold scavenging by bismuth melts coexisting with hydrothermal fluids. Geology, 36, 815.

Von Damm K.L., Buttermore L.G., Oosting S.E., Bray A.M., Fornari D.J., Lilley M.D., Shanks III W.C, 1997; Direct observation of the evolution of a seafloor 'black smoker' from vapor to brine. Earth and Planetary Science Letters.149, 101-111.

Vellutini. P., Piguet. P., 1994. Djibouti-Itinéraires géologiques. Ministère Français de Coopération et d'Action Culturelle à Djibouti. BCIMR et P.FA Ed, 289 pp.

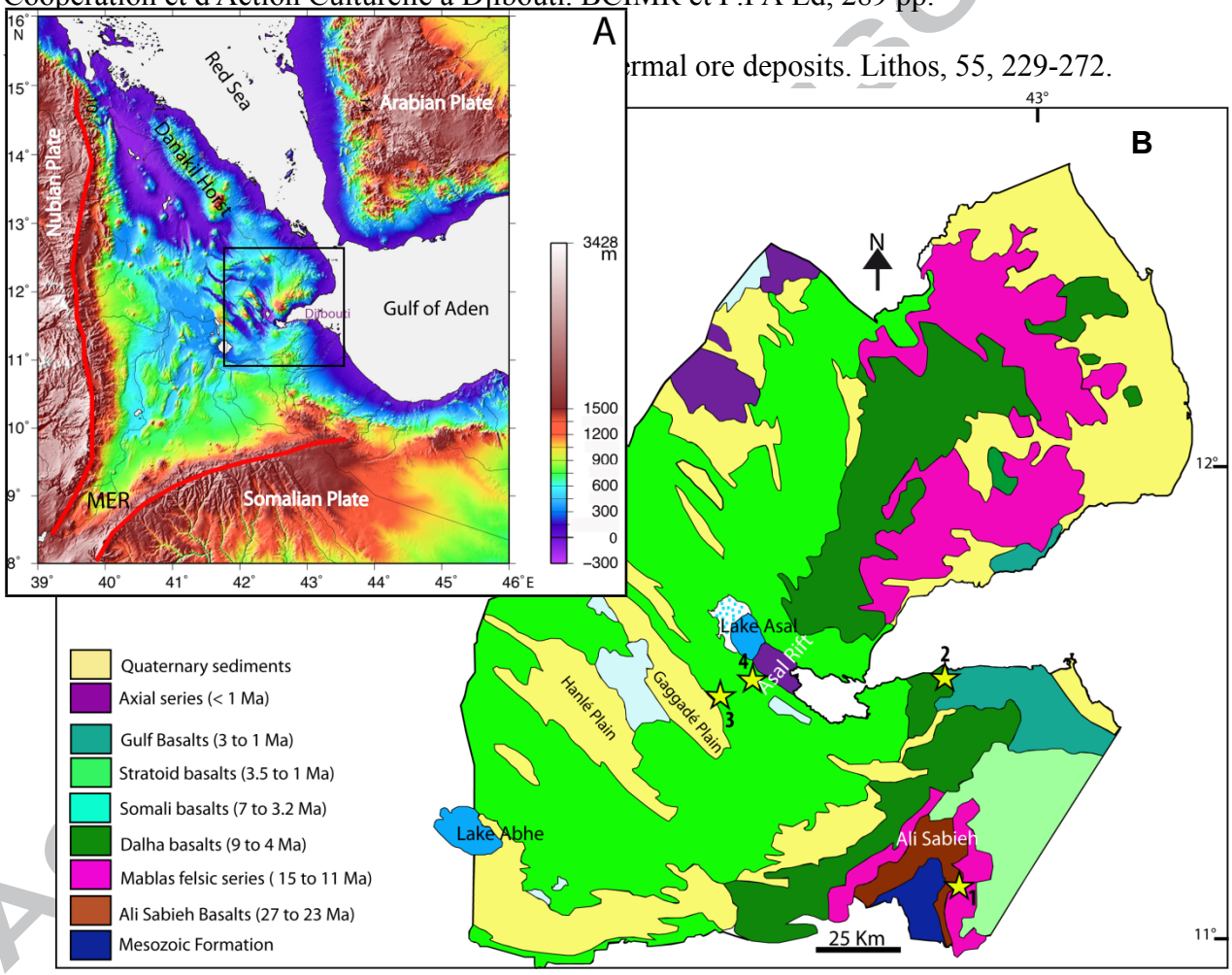

Fig. 1 :

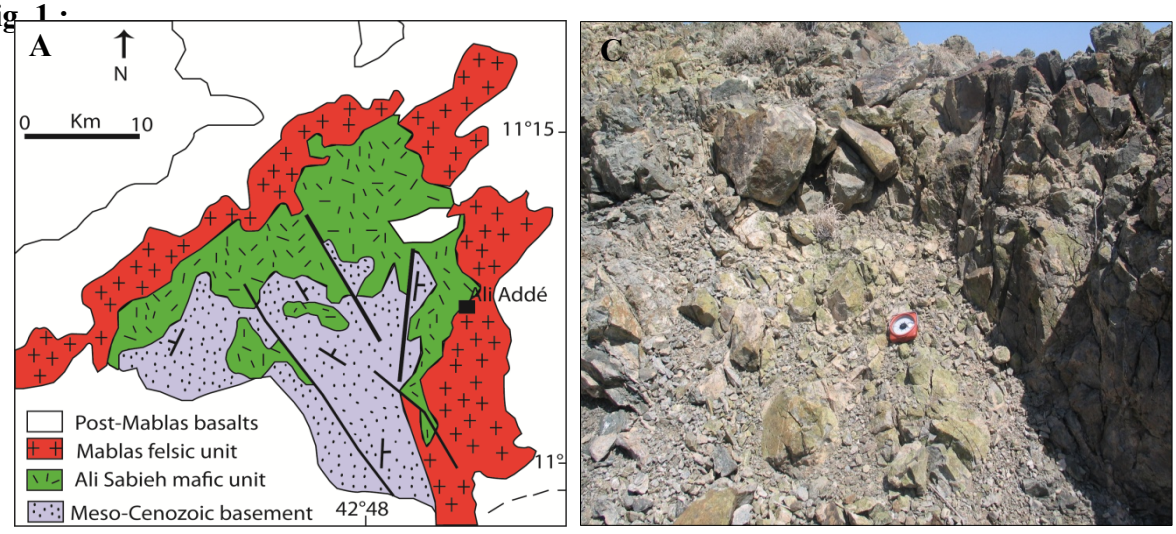

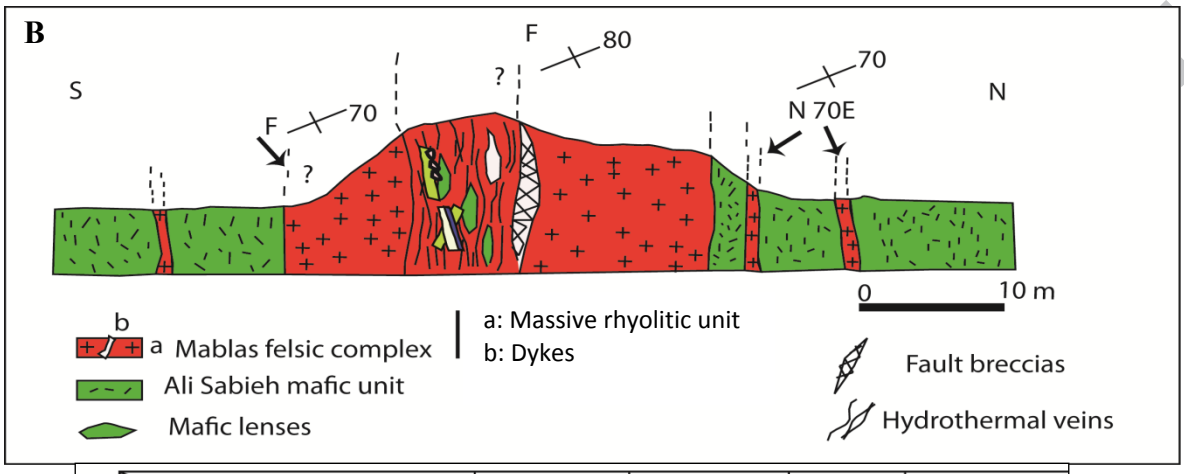

	Minerals \ Sites	Asa Leyta (< 3 Ma)	Hes Daba (< 3.3 Ma)	Arta (< 4 Ma)	Ali Addé (15 to 11Ma)
Hypogene minerals	Chalcopyrite $CuFeS_2$		+		+
	Pyrrhotite FeS	+	+		+
	Pyrite FeS_2	+	+	+	+
	Sphalerite (Zn,Fe)S		+		+
	Galena PbS		+		+
	Gold Au		+	+	
	Electrum AuAg		+	+	
	Argentite Ag_2S		+	+	
	Petzite Ag_3AuTe_2		+		
	Hessite Ag_2Te		+	+	
	Tetradymite Bi_2Te_2S				+
	Magnetite Fe_3O_4			+	
	Hematite Fe_2O_3		+	+	+
Supergene minerals	Chalcocite Cu_2S				+
	Covellite CuS		+		+
	Digenite Cu_9S_5		+		+
	Native Silver Ag		+		
	Native Copper Cu		+		
	Goethite FeO(OH)	+	+	+	+
	Bornite Cu_5FeS_4		+		
	Marcasite FeS_2		+		+
Gangue	Adularia $KAlSi_3O_8$	+	+	+	+
	Massive Quartz SiO_2	+	+	+	+
	Chalcedony SiO_2	+	+	+	+
	Carbonate $CaCO_3$	+	+	+	+
	Gypsum $CaSO_4\ 2(H_2O)$	+			

Fig. 2:

Fig. 3

Fig. 4:

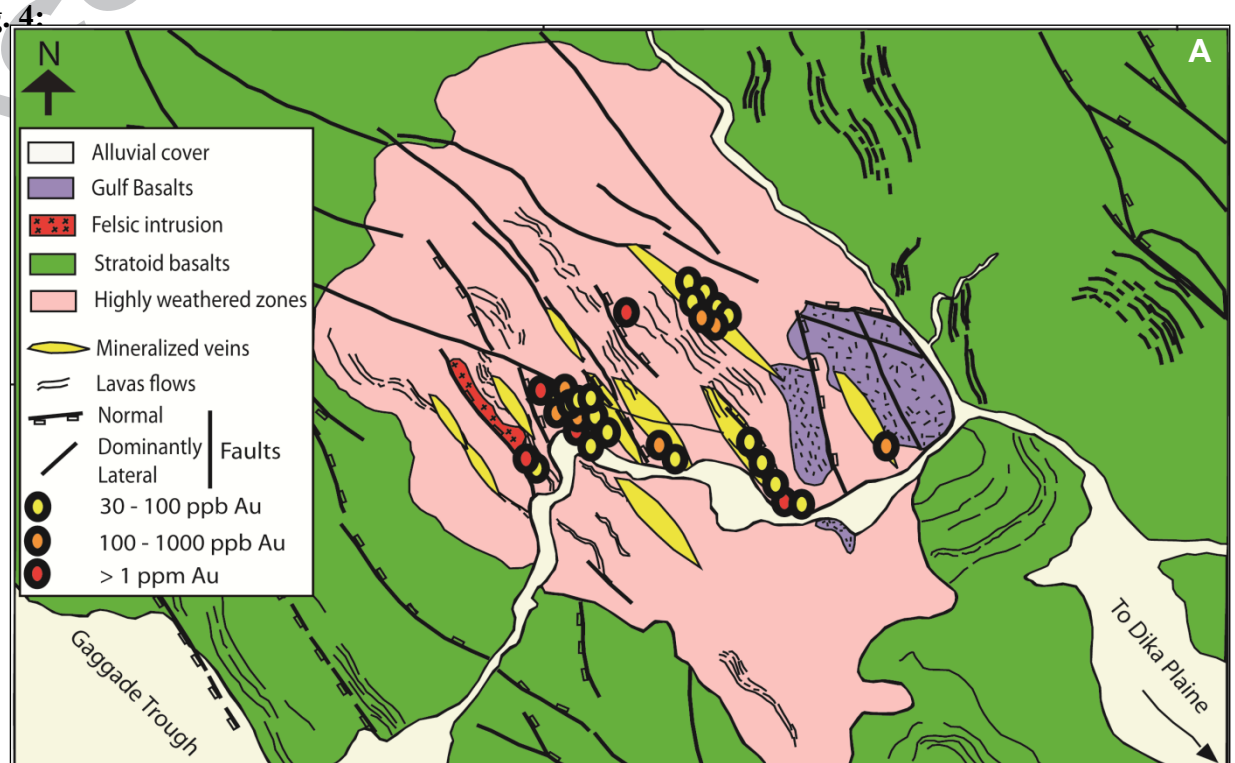

A

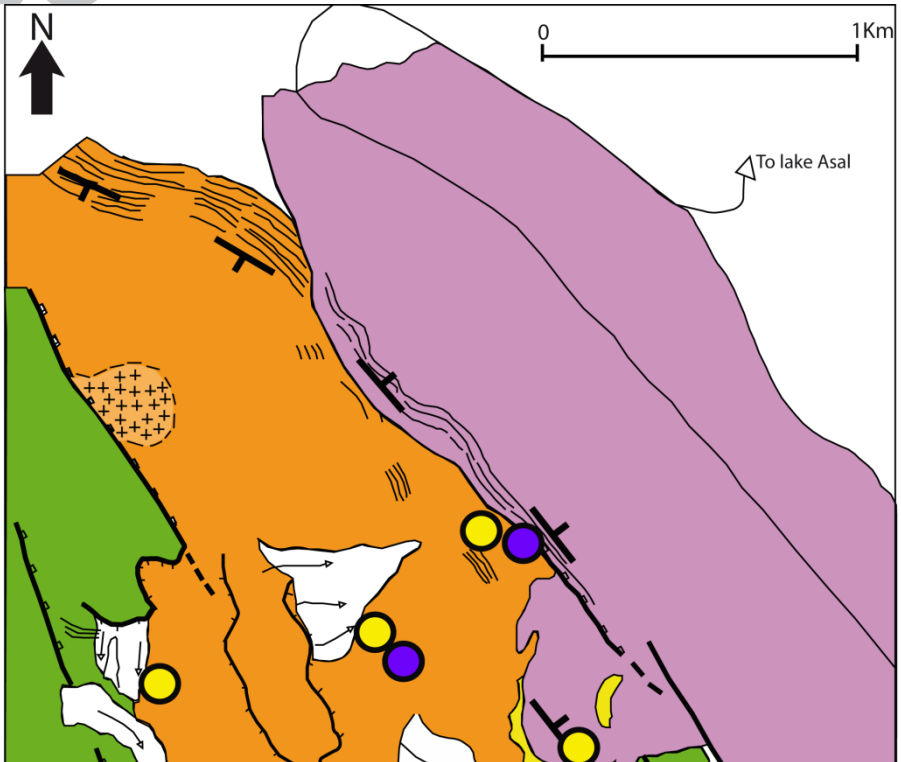

Fig.

Fig. 6:

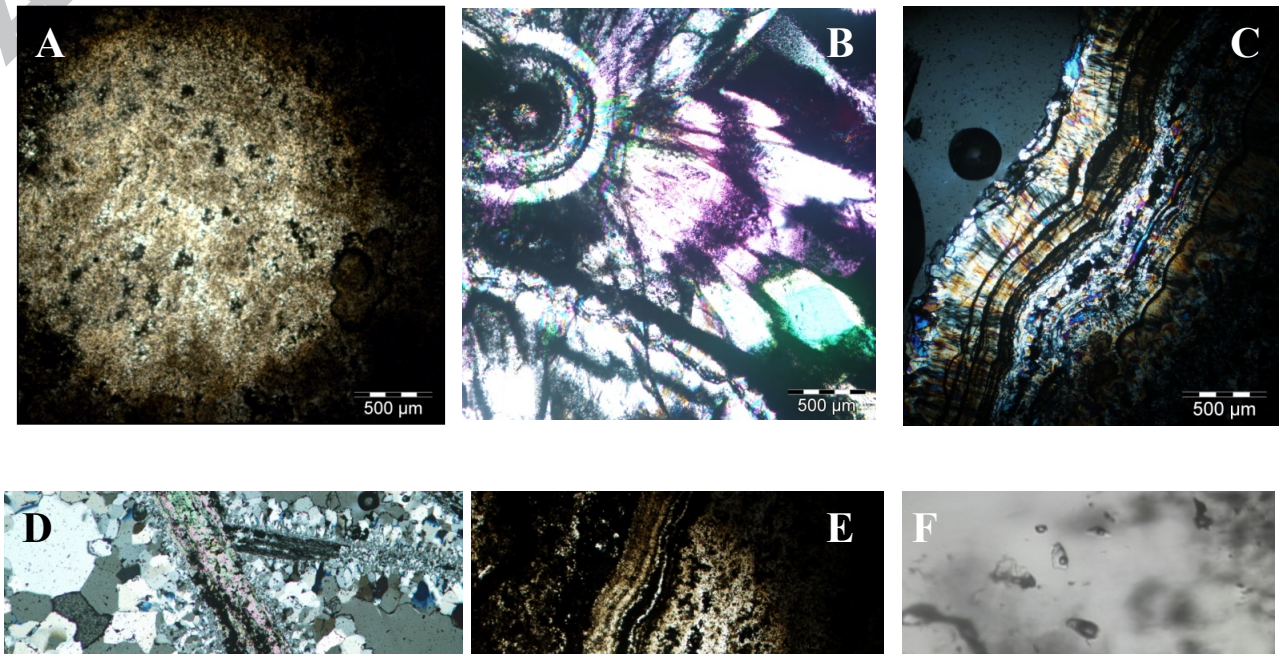

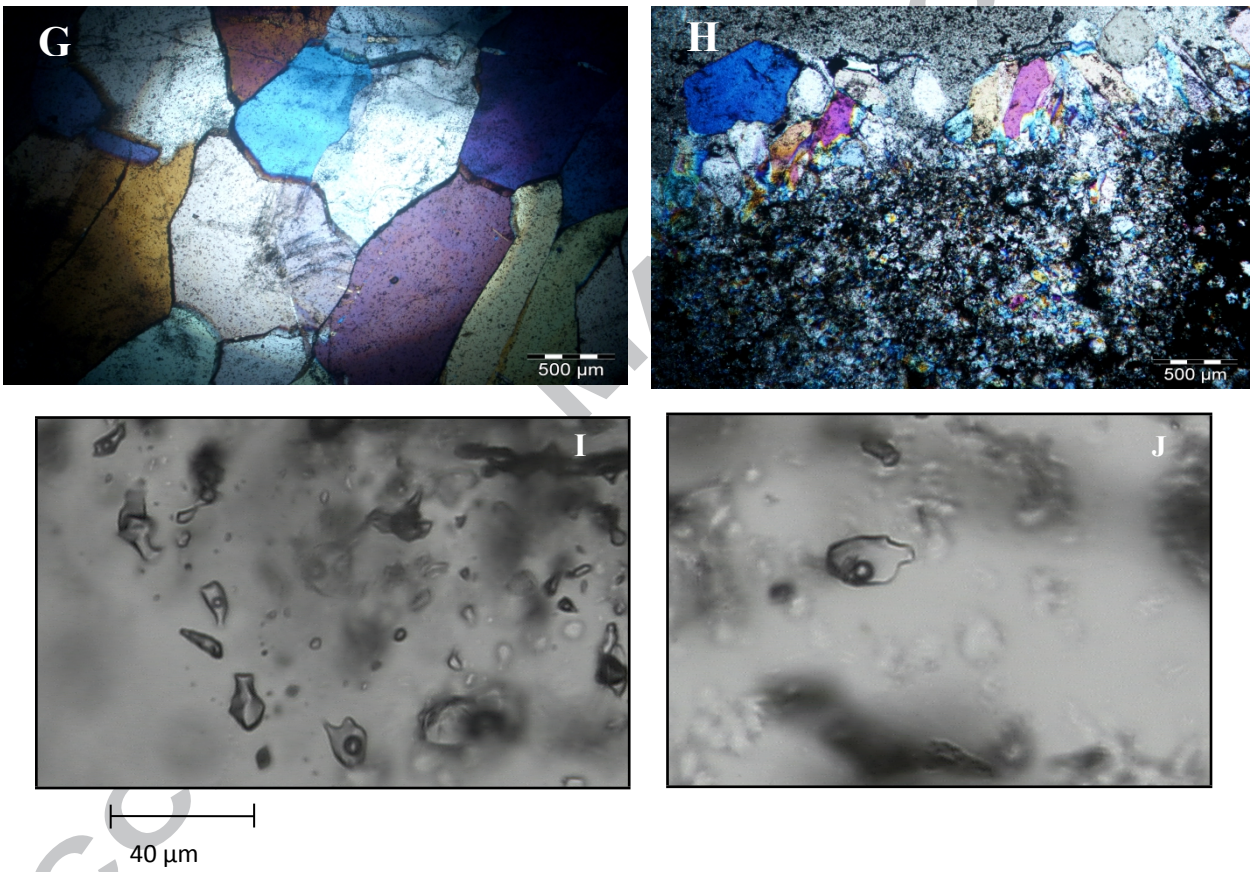

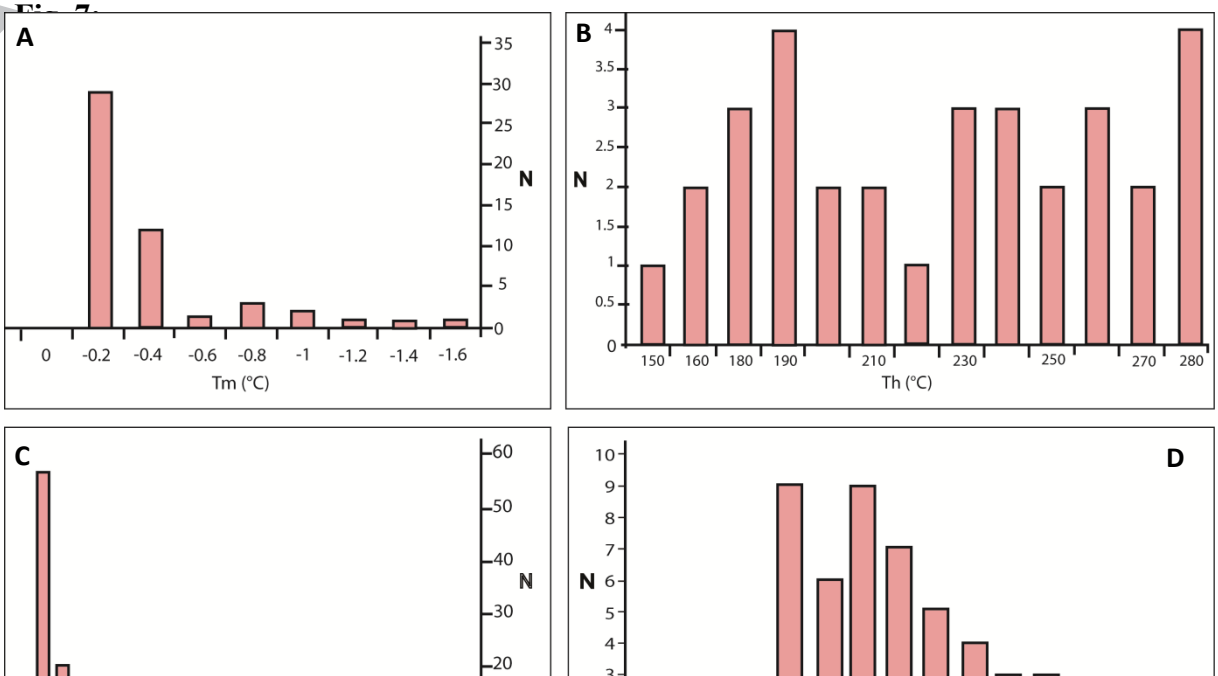

Fig. 8 :

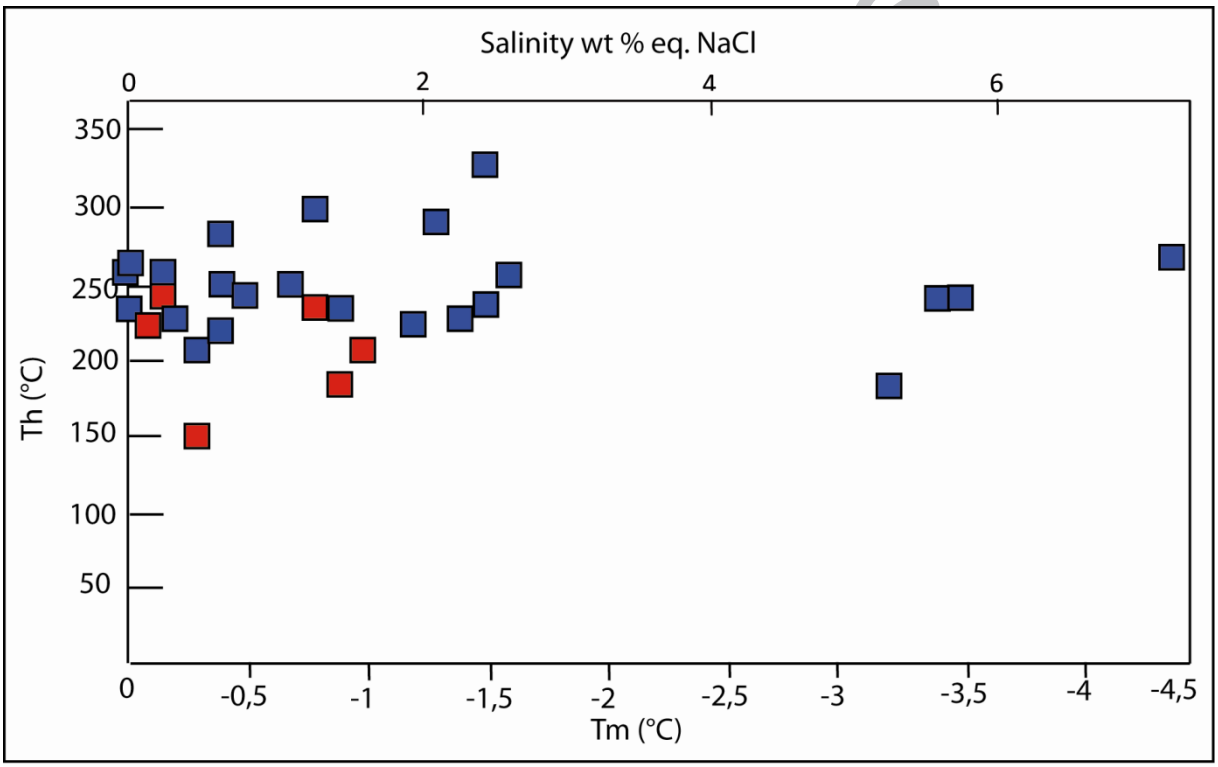

Fig. 9:

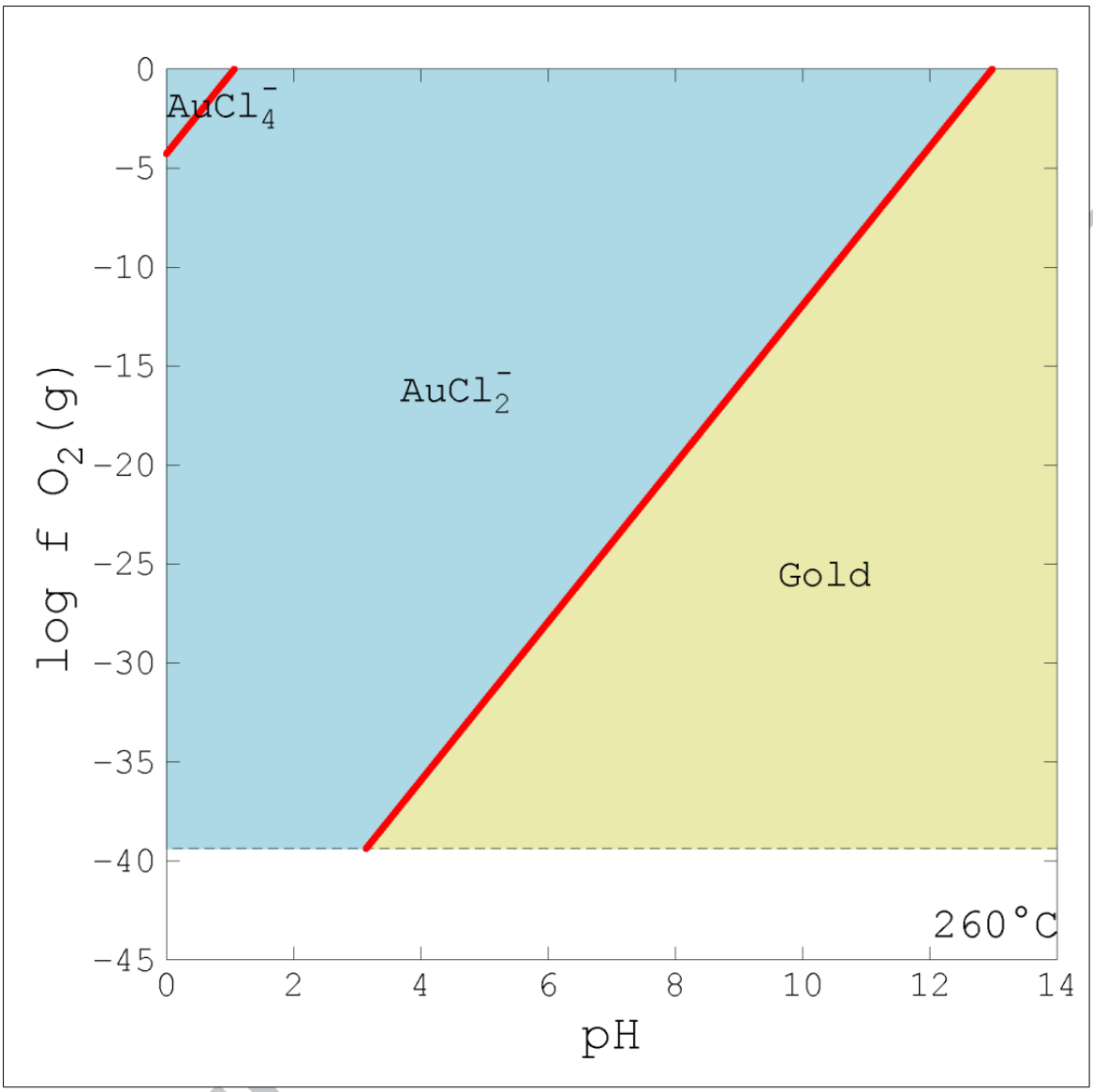

Fig. 10:

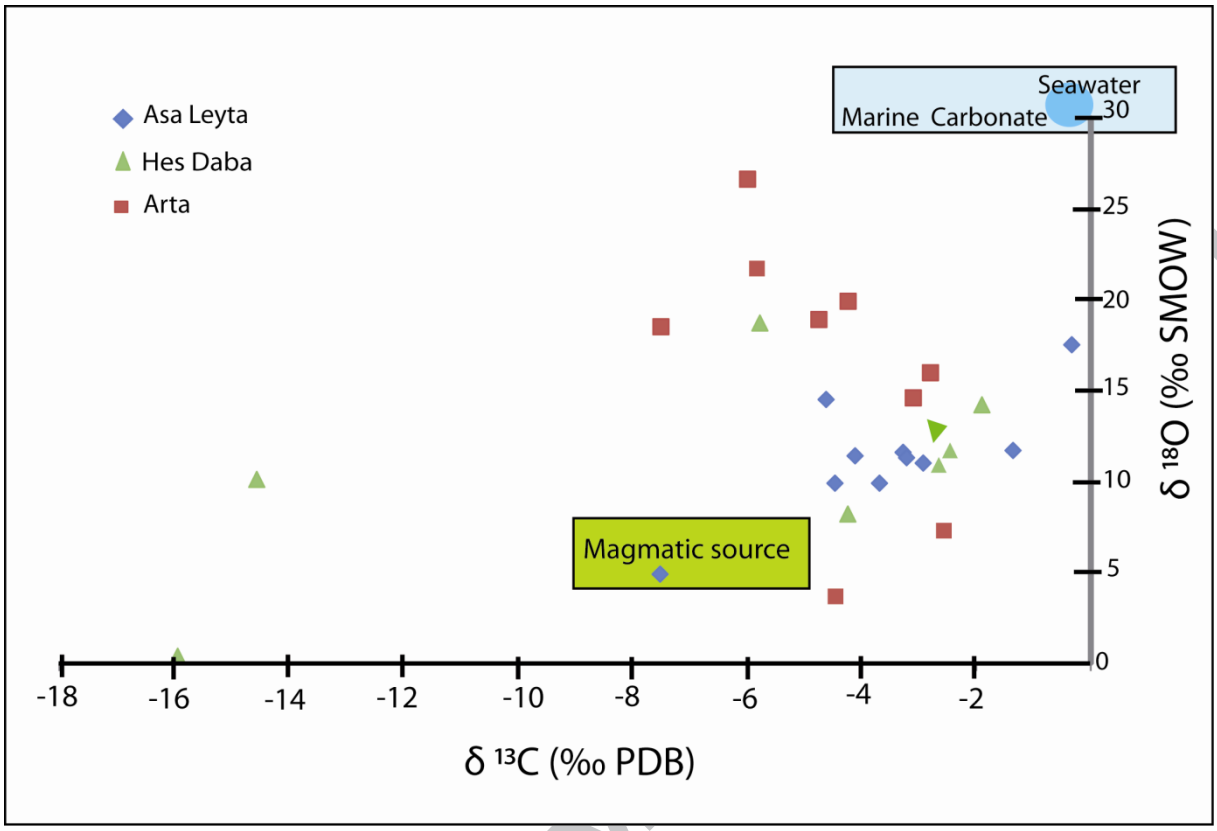

Fig. 11:

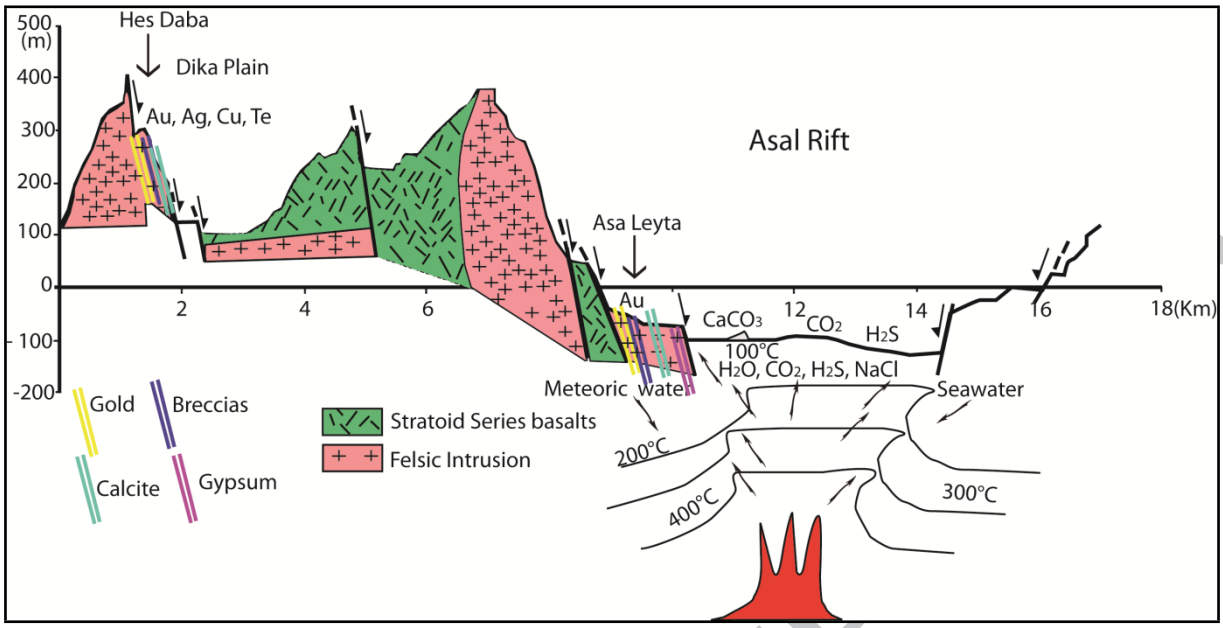

Fig. 12 :

Fig. 1: A: Digital elevation model (DEM) of the Afar rift with the Djibouti location. B: Schematical geological map of the Republic of Djibouti (SE Afar Triangle) after Vellutini and Piguet (1994). Yellow stars (and corresponding numbers) are the hydrothermal sites studied in this work. 1- Ali Addé; 2- Arta; 3- Hes Daba; 4- Asa Leyta.

Fig.2: A- Geological map of the South East of Djibouti. The black square corresponds to the Ali Addé hydrothermal site. **B-** Structural cross-section through the Mablas rhyolites. Mineralized facies occur mainly in chalcedony veins cross-cutting felsic volcanics. **C-** Stockwork of chalcedony veins hosted by felsic volcanic material**. D- E**: Elemental mapping of silver (**D**) and tellurides (**E**) grains (electron microprobe).

Fig. 3: Paragenetic sequences of the studied sites.

Fig 4: A – Schematical geological map of the Arta site and associated gold deposits. **B-** Banded chalcedony and adularia veins. **C**- Breccia-like veins. **D**- Hydrothermal calcite and breccia veins.

Fig 5: A - Schematical geological map of the Hes Daba site and associated gold deposits. **B-** Banded chalcedony and adularia veins. **C-** Breccia-like of carbonate veins. **D**- Hydrothermal calcite and breccia veins of calcite. **E**- Photomicrographs of calcite observed in samples from Hes Daba.

Fig. 6: A - Schematical geological map of the Asa Leyta and associated gold deposits. **B-** Banded chalcedony and adularia veins. **C-** Hydrothermal calcite and breccia veins.

Fig. 7: Photomicrographs of quartz textures observed in samples from Hes Daba and Ali Addé site. **A-** Microcrystalline quartz in the Stratoid Formation. **B** - Plumose quartz. **C-** Crustiform-Colloform –banded plumose, microcrystalline textures quartz (Hes Daba). **D-** Jigsaw texture replaced by lattice-bladed calcite (Hes Daba). **E** – Microcrystalline texture from Hes Daba site. **F-** Fluid inclusion types observed in samples from Hes Daba. **G-** Jigsaw texture (Ali Addé). **H-** Microcrystalline texture croscutted by jigsaw texture (Ali Addé). **I- J:** Fluid inclusion types observed in samples from Hes Daba.

Fig. 8: Histograms illustrating the ice melting temperature (Tm) and homogenization temperature (Th) of fluid inclusions from Ali Addé (**A-B**) and Hes Daba (**C-D**).

Fig. 9: Average homogenization temperature (Th) versus average melting temperature (Tm) for fluid inclusions from Hes Daba (blue square) and Ali Addé (red square) sites and estimated salinity.

Fig. 10: Diagram (y = O2 (g); x= pH) of gold (Au) with the following characteristics : Pressure = 1 atm; activity (a) main = 1e-10; a (Na+) = .6264; a (F-) = .0001579; a (Ca++) = .09631; a (Cu+) = 2.203e-6; a (Cl-) = .8491; a (Li+)= .0007709; a (Mg++) = .005659; a (SiO2(aq)) = .003845; a (NO3-)= .0007138; a (Sr++) = .0002659; a (Pb++) = 1.448e-6; a (Fe++) = .0001433; a (Al+++) = 3.706e-5; a (Zn++) = 1.774e-5; a (As(OH)4-) = 4.004e-7; a (B(OH)3) = .0004294; a (K+) = .02967; a (SO4--)= .01288

Fig. 11: Correlation between the isotopic values of oxygen and carbon of calcite for the three hydrothermal sites (Arta, Hes Daba and Asa Leyta).

Fig. 12: Cross-section between the Gaggadé and Asal rift system. This model shows the spatial relationship between mineralization, tectonics and felsic intrusions in the Djibouti Rift System. Hes Daba, Asa Leyta and Asal are controlled by tectonic activities.

Table 1: Carbon and Oxygen isotopes ratios of hydrothermal veins from Asa Leyta, Arta and Hes Daba (Cal: calcite; Qtz: quartz; Adu: Adularia)

Hydrothermal sites	Samples	Description of veins	C (‰, PDB)	O (‰, SMOW)
Asa Leyta	Cal 147	Cal	-2.9	11
	DJ-01-08B	Qtz- Cal	-3.3	11.6
	DJ-02-08B	Cal	-1.4	10
	DJ-76-08-A3	Qtz- Cal	-4.5	9.9
	DJ-23-08-2	Qtz- Cal	-3.2	11.3
	DJ-24-08A	Qtz- Cal	-4.1	11.4
	DJ-25-08C	Cal	-0.3	17.5
	DJ-09-09	Qtz- Cal	-3.7	9.9
Arta	DJ-12-07-A	Qtz- Cal	-4.7	18.9
	DJ-11-08A	Qtz- Cal	-2.8	15.7
	DJ-30-08	Qtz- Cal	-6	15.7
	DJ-36-08	Qtz- Cal	-2.6	7.3
	DJ-61-08	Qtz- Cal	-7.5	18.5
	DJ-03-09A	Qtz- Cal	-3.1	14.6
	DJ-55-09-1	Qtz- Cal	-4.2	19.9
	DJ-16-10 MW	Cal	-2.6	10.7
	DJ-18-10	Qtz- Cal	-4.5	3.7
	F1HN140	Qtz- Cal	-5.8	21.7
	1-F61N140	Qtz- Cal	-1.1	12.3
Hes Daba	DJ-70-08	Qtz- Cal	-5.77	18.7
	F1SE	Qtz- Cal	-14.55	10.1
	F1SE Cu	Qtz- Cal	-1.9	14.2
	DJ-10-09C	Qtz-Cal	-4.24	8.2
	F3B	Qtz-Cal	-15.93	0.4
	2F1NOA	Qtz-Cal- Adu	-2.46	11.7
	3F1NO1	Qtz-Cal	-2.65	10.9

Table 2: Results of the fluid geochemistry (mg/kg) of the Asal 3 Geothermal field (D'Armore et al., 1998).

pH	4,9
Na	37452
K	7273
Ca	23928
Mg	37
Cl	106000
SO4	32
SiO2	520
HCO3	66
Li	31
F	7
NH3	9,1
Zn	3,1

Pb	3,4
Fe	6,7

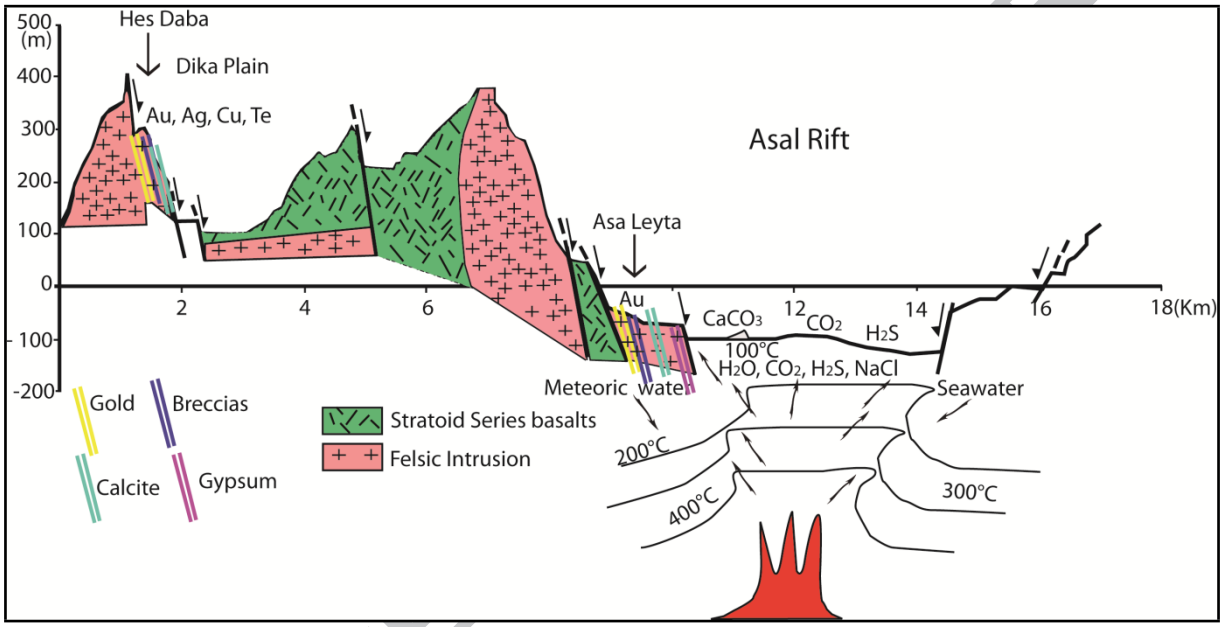

Figure: Correlation between mineralization, tectonic and felsic intrusions in the SE Afar Rift system.

- Au-Ag-Bi-Te minerals deposits on the edge of the Asal rift system (Djibouti)
- Microthermometric measurements and stable isotopes (C, O) were made on hydrothermal veins (e.g. quartz and carbonate veins) from the SE Afar Rift (Djibouti).
- Mean homogenization temperature ranges from 150°C to 340°C and ice-melting temperatures range from -0.2° to - 1.6°C and contain 0.35 to 2.7 eq. wt. % NaCl.

- $\delta^{18}O$ and $\delta^{13}C$ values from calcite range from 3.7 to 26.6 ‰ and -7.5 to 0.3‰, respectively.
- The most common textures of quartz are microcrystalline, jigsaw, plumose, crustiform and colloform.
- Three types of fluids have been identified in the SE Afar Rift: magmatic, meteoric and seawater fluids.